ANNALI DI GEOFISICA, VOL. 41, N. 1, April 1998

# Upper crustal structure in the Potenza area (Southern Apennines, Italy) using *Sp* converted waves

**Donat Demanet**([1]), **Lucia Margheriti**([2]), **Giulio Selvaggi**([2]) **and Denis Jongmans**([1])
([1]) *Laboratoires de Prospection Géophysique, Liège University, Liège, Belgium*
([2]) *Istituto Nazionale di Geofisica, Roma, Italy*

**Abstract**
In this paper we analyse the records of the two Potenza seismic sequences (Southern Apennines, Italy) which occurred in 1990 and 1991, in order to obtain information on the upper crustal structure in this area. The hypocentral depths are mainly concentrated below 10 km which is the supposed upper limit of the crystalline basement. The seismograms recorded at temporary arrays deployed during the two sequences clearly show on the vertical component, an intermediary phase between the *P* and *S* waves. For the investigated epicentral distances (less than 30 km) the delay between this secondary phase and the direct *S* wave arrival is almost constant at each station, suggesting that the observed intermediary phase might be an *S* to *P* conversion at a discontinuity shallower than the hypocentral depth. This interpretation has been supported by polarisation analysis and numerical modelling results. Considering the regional geological structure, these latter have also shown that the interface generating strong converted waves could be the top of the Apulian carbonate platform overlaid with recent clay deposits and flysch sediments. 1D inversion of the travel-time data was performed in order to evaluate a local vertical upper crustal profile.

**Key words** *Southern Apennines – upper crustal structure – Sp converted waves – inversion*

## 1. Introduction

The geological structure of the Southern Apennines is very complex and its tectonic history is still a strongly debated question (see, *e.g.*, the recent review of Marsella *et al.*, 1995). On the other hand, the recent discovery of oil fields in this fold-and-thrust belt (D'Andrea *et al.*, 1993; Roure and Sassi, 1995) has increased the interest in investigating the area and understanding its tectonic evolution. The exploration is however limited by the reservoir depth (more than 4 km) and the poor quality of the reflection seismic data (D'Andrea *et al.*, 1993).

In other respects, the Southern Apennines are characterised by a relatively high seismic activity with large earthquakes ($M = 7$) occurring during historical times and numerous moderate magnitude seismic sequences. Two of such sequences occurred in 1990 and 1991 in the Potenza area where accurate digital seismic data were collected by temporary networks. The data analysis allowed us to locate the aftershocks and to show that earthquakes occur along an E-W striking vertical plane. This high seismic activity around Potenza also provides an opportunity to study the upper crustal structure of the area through sampling

*Mailing address*: Dr. Donat Demanet, Laboratoires de Prospection Géophysique, Liège University, Bat. B19, 4000 Liège, Belgium.

by different seismic phases including converted waves. The aim of this paper is to investigate the geological structure beneath the seismological stations from local earthquake records and to assess the potentiality of the method to the case of the Southern Apennines.

## 2. Geological and seismotectonic outline

Southern Apennines are a tectonic stack of Mesozoic-Paleogene sedimentary basins and carbonate platform rock units, emplaced since the Late Miocene and coeval with the opening of the Tyrrhenian basin (Malinverno and Ryan, 1986; Dewey *et al.*, 1989; Patacca and Scandone, 1989). During the Plio-Pleistocene, extensional tectonics related to the opening of the Tyrrhenian basin progressively replaced the compressional regime and affected the whole mountain belt, with the development of Plio-Pleistocene grabens. In the present time, a NE-SW extension is clearly shown by normal fault earthquakes and borehole breakout (Anderson and Jackson, 1987; Frepoli and Amato, 1997; Montone *et al.*, 1997).

Four main geological units are found in the Southern Apennines (Mostardini and Merlini, 1986). They are, from west to east, the Liguride Complex, the Apenninic carbonate platform, the Lagonegro deposits and the inner and outer Apulian platform (fig. 1a,b). The Liguride Complex, mainly pelitic sediments of an internal paleogeographic realm (Jurassic to Early Tertiary), is thrust over the Apenninic carbonate platform (middle Trias to Lower Miocene). Both units are thrust over the Lagonegro deposits. These latter are generally divided into limestones and marls lower sequence (the older one – middle Trias to Lower Cretaceous) and in an upper sequence of incompetent clays (Upper Cretaceous to Lower Miocene). The Lagonegro basin is thrust over the inner Apulian carbonate platform (fig. 1b), which is strongly deformed and thrust over the outer undeformed Apulian carbonate platform, the latter constituting the orogenic foreland. During the building-up of the chain, some intra-décollement phenomena might have occurred inside the Lagonegro deposits. Other younger units are present in the studied area (fig. 1a,b): the Irpinian flyschs of Miocene age and recent (Pliocene to Holocene) deposits, including the Bradano trough in the foredeep. During the last compressive phase occurring at the end of the early Pliocene, flysch sediments and a part of the Lagonegro basin thrusted over the Pliocene foredeep, above the Apulian platform. The juxtaposition of argillaceous sediments on the Apulian platform is a typical sedimentary trap for oil storage.

Large magnitude crustal earthquakes, up to $M = 7$, occur within this tectonic framework with decades of time interval. They are concentrated along the highest elevation regions of the Apenninic belt. A more frequent moderate size seismicity is present and when recorded by dense digital local networks, provides the opportunity to investigate the crustal structures through the seismological information contained in the earthquake waveforms. In this paper, we show that converted phases at crustal discontinuities can be efficaciously recognised and modelled to recover the depth of such discontinuities. This approach is particularly well suited for the Potenza area (fig. 1a,b), a small region within the Southern Apennines, where frequent seismicity provides a large amount of data and where oil exploration has been successfully carried on in the past few years (D'Andrea *et al.*, 1993; Roure and Sassi, 1995). We concentrate on the last two seismic sequences which occurred in 1990 and 1991, that have been recorded by local networks.

The $M_w = 5.7$ Potenza mainshock occurred on May 5, 1990 at 7:21 GMT and was located 40.64°N and 15.86°E, at 15 km depth. The focal mechanism shows an almost pure strike-slip solution (Azzara *et al.*, 1993; Ekström, 1994). The aftershock sequence ended after about one month and was recorded by a micro-earthquake digital network, installed a few days after the mainshock in the epicentral area (fig. 2). The network was equipped with 2 three-component and 4 vertical component short period remote digital stations and the incoming signals were digitised at 125 sps. All the stations were located on Lagonegro unit sediments. The epicentral map (fig. 2) shows

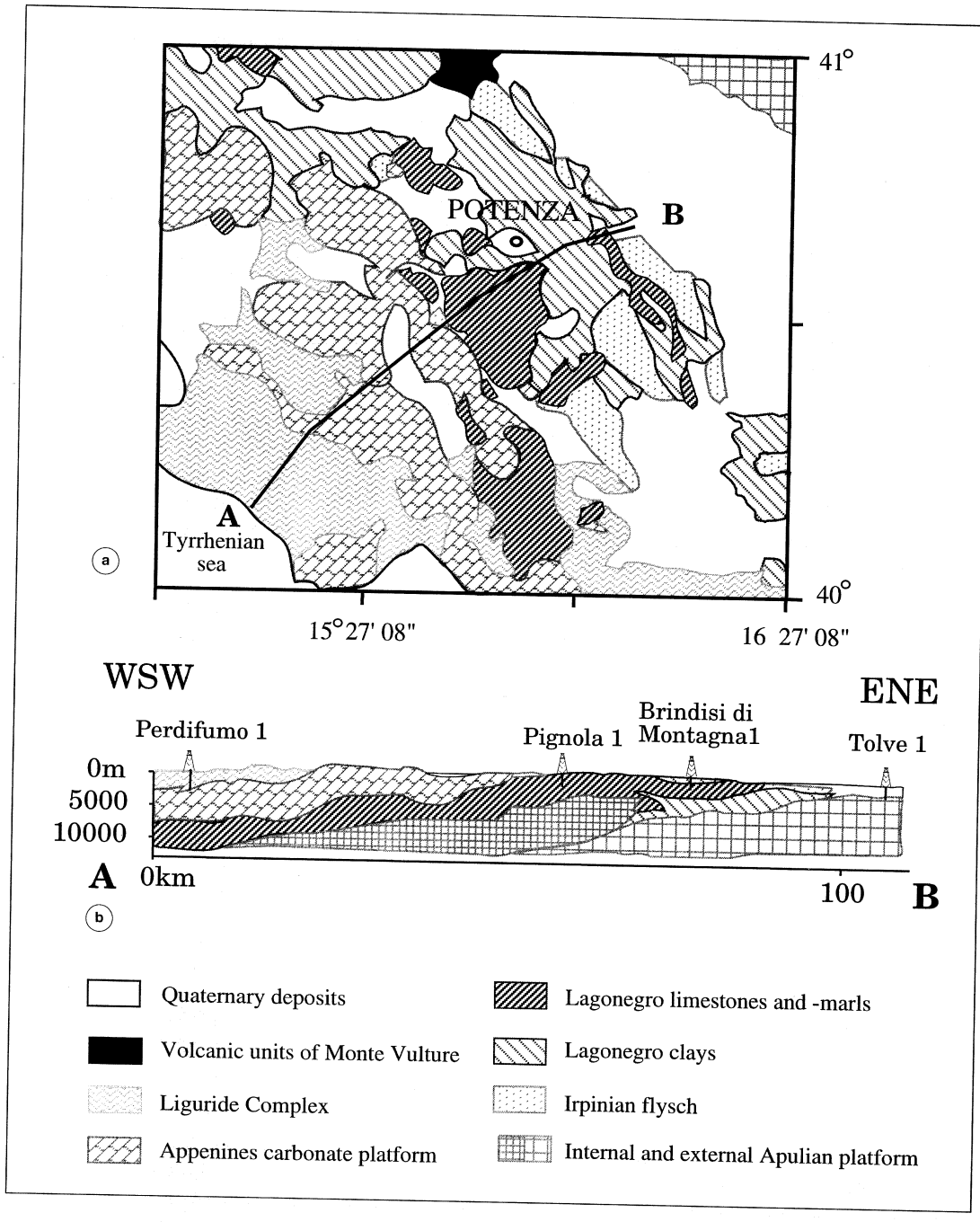


**Fig. 1a,b.** a) Geological sketch of the Southern Apennines; b) geological section along the A-B profile on the map (simplified from Mostardini and Merlini, 1986).

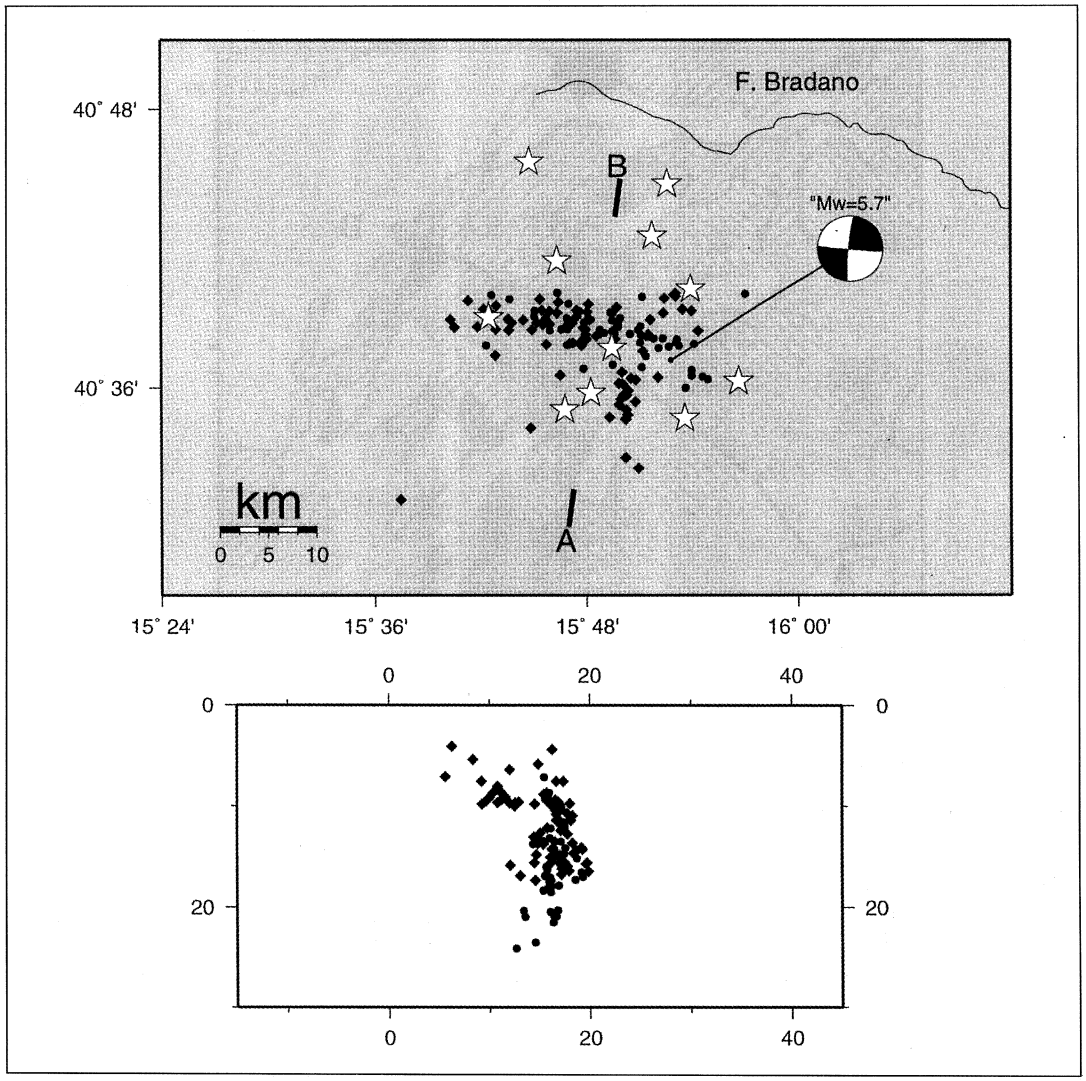


**Fig. 2.** Locations of the Potenza 1990 (solid circles) and 1991 (solid diamonds) aftershocks. Above: map view, also shown are mainshock fault plane solution and station locations (stars); below: cross-section (A ~ 0 km, B ~ 35 km).

that the earthquakes are comprised in an east-west striking zone which extends for about 15 km, with a small dispersion at the edges of the network (Azzara *et al.*, 1993). The hypocentral depths are mainly concentrated between 15 and 25 km (fig. 2). Mainshock fault plane solution and aftershock distribution revealed the presence of a 15 km long right lateral strike slip fault. The May 26, 1991 $M_w$ = 4.8 earthquake occurred within a few kilometers from the 1990 mainshock, showing a similar focal mechanism (Ekström, 1994). The ING in-

stalled a digital seismic network in the epicentral area. The six three-component digital stations allowed us to locate more than 50 aftershocks with magnitudes ranging from 2.0 to 3.0 during 20 days of recording. The epicentral map (fig. 2) shows that the seismic activity affected an area of 40 km$^2$ elongated in east-west direction that clustered slightly westward the 1990 sequence (Azzara *et al.*, 1993). The hypocentral depths are mostly confined between 10 and 15 km. The aftershocks of the 1990 and 1991 sequences depict an east-west 20 km long fault. In section, the hypocenter distribution shows an almost vertical fault from 10 to 25 km in depth. Both seismic sequences were located with the same *P* wave velocity model, derived from Mostardini and Merlini (1986); this model has also been used for synthetics (model 1).

## 3. Secondary phase analysis

The seismograms recorded at the temporary arrays, relative to the 1990 and 1991 sequences described above, clearly show on the vertical component a secondary phase out of the direct *P* and *S* waves. This secondary arrival is often impulsive with a frequency content generally lower than the direct *P* wave arrival. The examples in figs. 3 and 4 show a secondary phase having amplitude greater then the direct *P*, this is not always the case. To identify the nature of this arrival we first picked its arrival time to see if there was any systematic behaviour. We noticed that the delay time of the secondary phase, relative to the *P* arrival, was not correlated with earthquake hypocentral depth or distance. On the contrary, the delay between the secondary phase and direct *S* wave arrival was almost constant at each station, suggesting that the observed secondary phase might be an *S* to *P* conversion at a discontinuity shallower than the hypocentral depth.

To gain confidence in our identification, we carried out a polarisation analysis, using covariance matrix decomposition (Jurkevics, 1988) and filtering the signals between 1.5 and 5 Hz, to determine the direction of polarisation of the secondary phase. In the Z-NS-EW space the covariance matrix $M$ is

$$M = \begin{vmatrix} \mathrm{Var}(EW) & \mathrm{Cov}(NS, EW) & \mathrm{Cov}(Z, EW) \\ \mathrm{Cov}(EW, NS) & \mathrm{Var}(NS) & \mathrm{Cov}(Z, NS) \\ \mathrm{Cov}(EW, Z) & \mathrm{Cov}(NS, Z) & \mathrm{Var}(Z) \end{vmatrix}$$

The three eigenvalues $l_1\, l_2\, l_3$ are computed using a series of 0.4 s (50 samples) time windows partially overlapped along the seismograms. The polarisation direction corresponds to the direction of the eigenvector $(u_{ew}, u_{ns}, u_z)$ relative to the largest eigenvalue $l_1$ of the covariance matrix

$$P_{az} = \tan^{-1} u_{ew}/u_{ns}.$$

We also evaluated the rectilinearity and the shear angle, to better identify and discriminate phase arrivals. Rectilinearity is defined as

$$R = 1 - [(l_2 + l_3)/2\, l_1]^n$$

while the shear wave angle is

$$S_w = \cos^{-1}(u_z)$$

which is the angle between the largest eigenvector and the vertical axis (the dip of the polarisation). As we are looking for a secondary *P* arrival supposed to have the same azimuth as the direct *P*, we expect rectilinearity close to 1 and a low shear angle. Figure 4 shows an example at CAR9 station where the *P*, *Sp*, and *S* arrival are clearly identified by $R$ and $S_w$ values. The *P* wave polarisation is quite stable in the frequency window between 1.5 and 5 Hz and close to the back-azimuth of the event (BAZ = 142). Polarisation analysis made us confident on the identification of the secondary phase as an *S* to *P* conversion (*Sp*) at a crustal discontinuity.

In order to enable an easy and quick picking of *Sp* phases, the *RZ* (radial × vertical) product was computed. As shown by Jacob and Booth (1977) and applied by Regnier *et al.* (1994), the *RZ* product enhances coherent rectilinear motions and attenuates waves with elliptical particle motion. Arrival times of the three

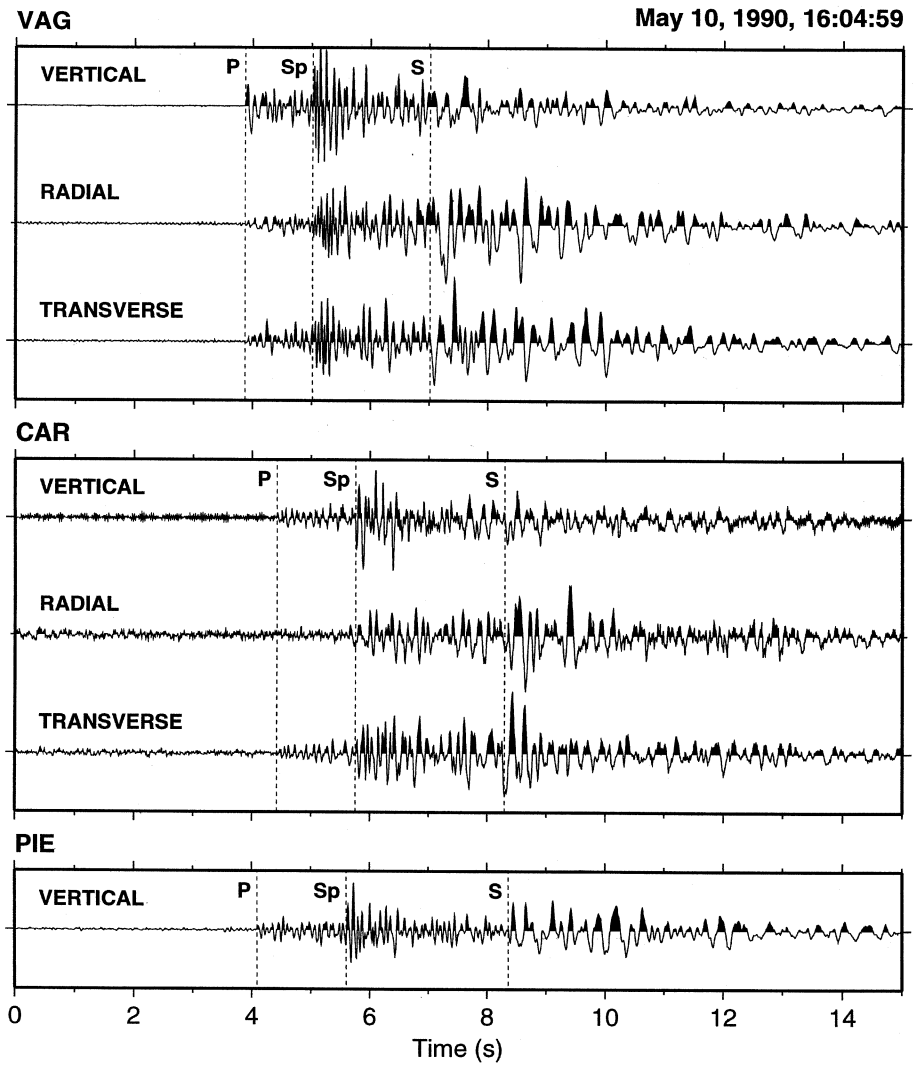


**Fig. 3.** Examples of observed seismograms recorded at three stations of the network during the earthquake of May 10, 1990. Besides *P* and *S* arrivals, the data systematically show an intermediate phase (*Sp*) which is more important on the vertical component than on the horizontal ones.

phases (*P*, *Sp* and *S* waves) have been picked on all the records exhibiting a good signal-to-noise ratio. This work led to a total of 337 arrival time values determined from 115 signals recorded at 10 stations for 50 seismic events. All the signals were processed by two people and the results were cross-checked. If the measurement discrepancy was too high, the data were rejected. Generally, 12 to 23 events were recorded at each station (see table I), except at PIE, LIF and SLN (2, 3 and 1 events, respectively).

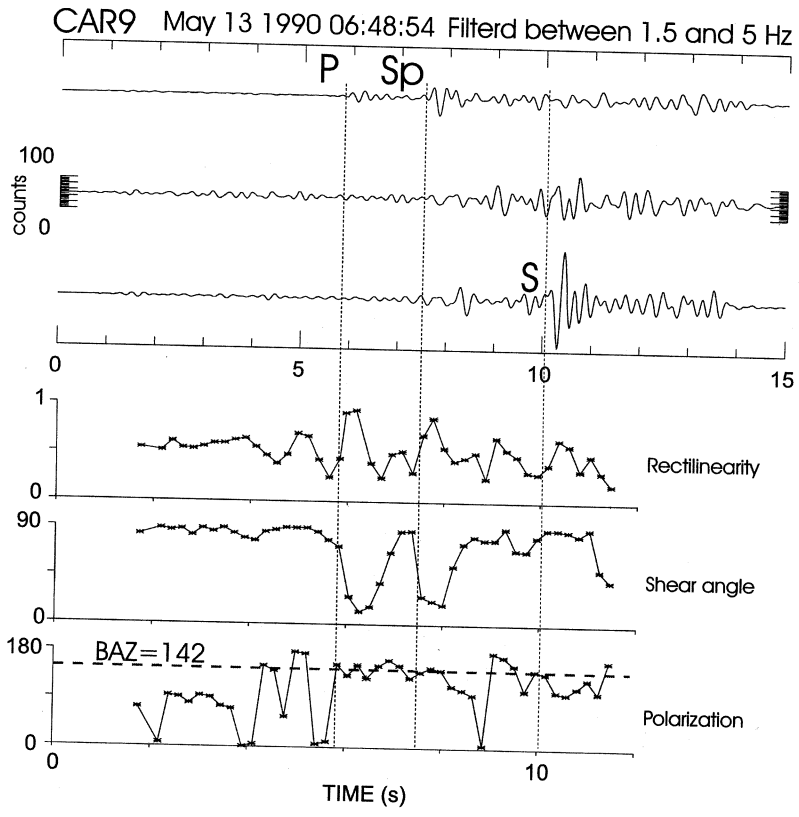


**Fig. 4.** Example of polarisation analysis performed on the seismograms rectilinearity, shear-wave angle and polarisation angle are calculated on running windows along the seismograms. The main 3 phases are identified by rectilinearity picks. Low shear angles indicate *P* and *Sp* phases, high shear angles *S* phases. Note that *P* and *Sp* directions of polarisation are similar as expected for these phases and close to the BAZ of the event.

**Table I.** Mean and standard deviation of *S-Sp* times for all the stations.

| Station | Number of events | Mean *S-Sp* times (s) | Standard deviation *S-Sp* times (s) |
|---|---|---|---|
| PIE | 2 | 2.70 | 0.09 |
| CAR | 23 | 2.55 | 0.18 |
| CZS | 13 | 2.22 | 0.27 |
| SLN | 1 | 2.11 | – |
| PGC | 16 | 2.08 | 0.33 |
| BRI | 15 | 2.00 | 0.34 |
| VAG | 14 | 1.89 | 0.27 |
| PIG | 12 | 1.59 | 0.29 |
| GIU | 13 | 1.47 | 0.28 |
| LIF | 3 | 1.42 | 0.68 |

Figure 5 plots the arrival times *versus* the source-station distance. The top-left graph of this figure shows the data for all the stations, while the other graphs display the data for 8 separate stations. For *P* waves, data scattering is similar on all the graphs. On the contrary, scattering for *Sp* and *S* waves appears to be more important when gathering all the stations together. This reflects the higher sensitivity of these two seismic phases to local geological conditions beneath the stations. Looking at the data in fig. 5, one can observe that the time difference between *S* and *Sp* waves varies with the station location. This *S-Sp* relative time depends on the depth of the discontinuity at which shear waves are converted and can then be used for investigating the local crustal structure.

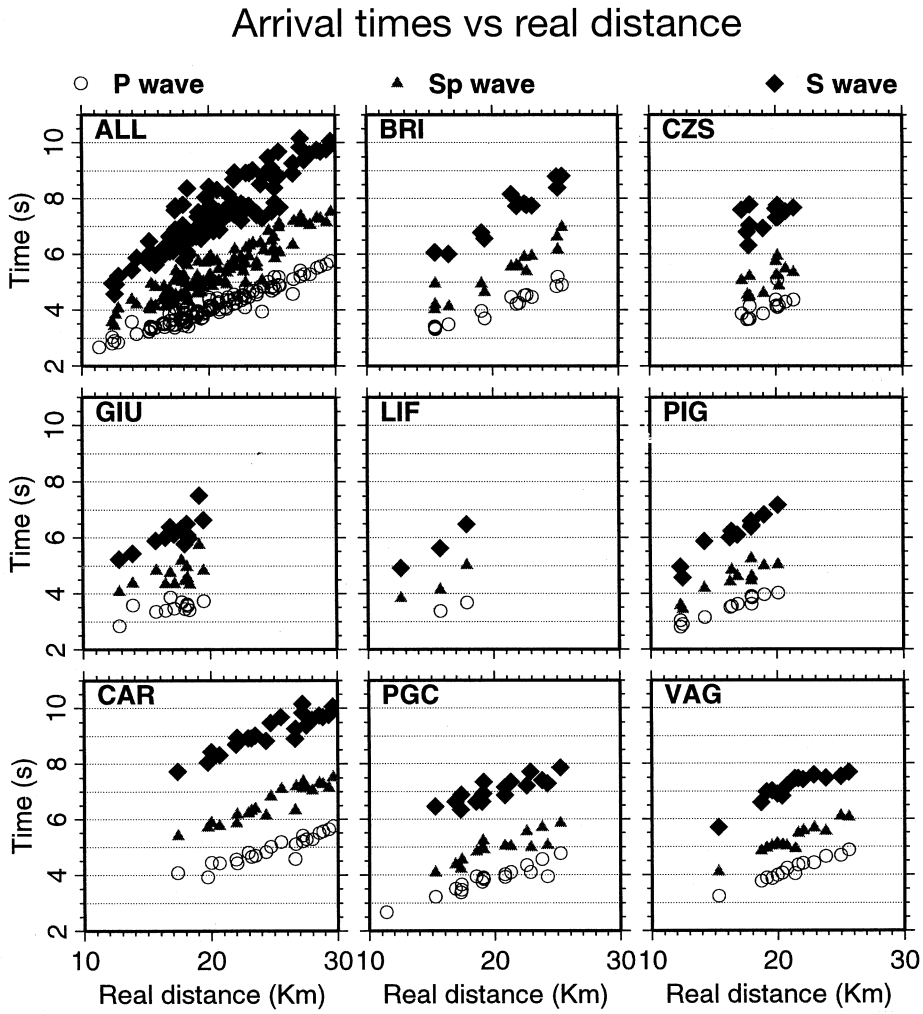


**Fig. 5.** Arrival times for the different phases (*P*, *Sp* and *S* waves) at different stations plotted over hypocentral distance. The first plot refers to all the stations together while the others show the arrival times station by station.

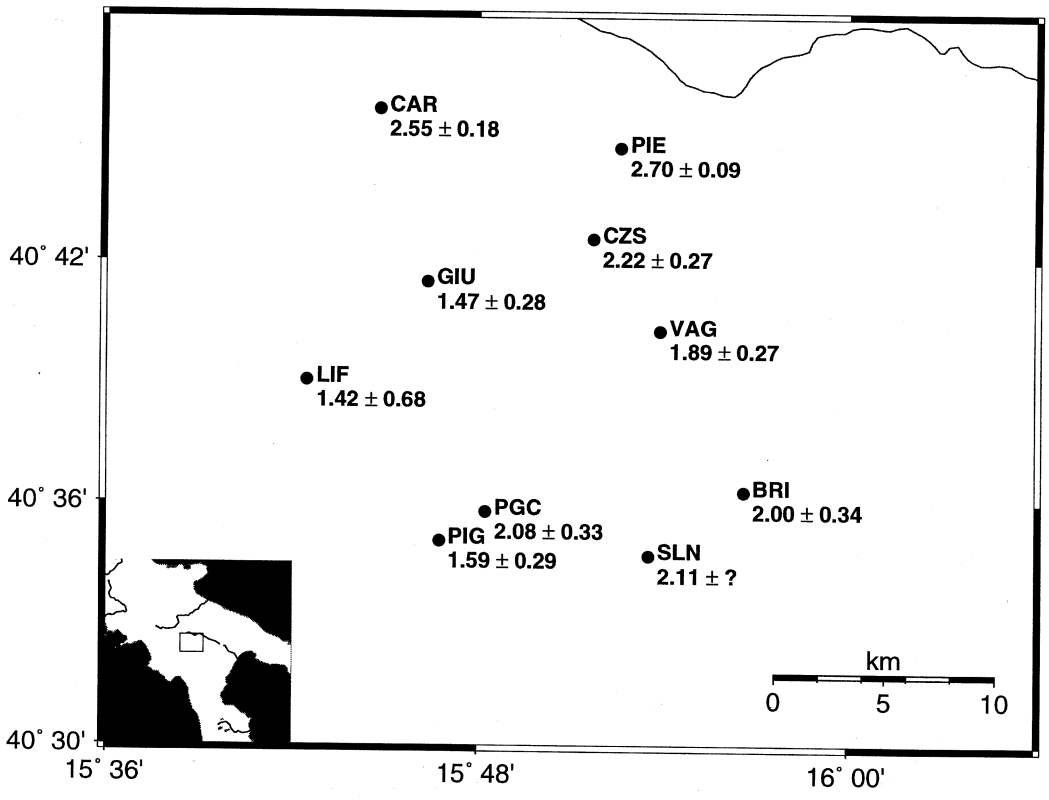


**Fig. 6.** Average values of *S-Sp* arrival times and standard deviations at the stations.

First, we checked that there was no obvious *S-Sp* time dependence on the source distance or depth, then we computed the mean value and the standard deviation at each station. The results are presented for the ten stations in table I and in fig. 6. At SLN, just one datum was available.

The mean *S-Sp* time values are between 1.42 s and 2.70 s, with a standard deviation ranging usually from 0.18 s and 0.34 s. The general trend is an increase in *S-Sp* times from the SW to the NE with some exceptions (PGC). From the available information (fig. 1b), high *S-Sp* values correlate with a relative deeper Apulian platform and with the more conspicuous presence of the clay part of the Lagonegro formation.

## 4. Synthetics

In order to study the origin of these converted waves, we modelled the radiation of a source point using the discrete wave number method (Bouchon, 1981). The assumed focal mechanism is a dextral strike-slip with the hypocenter located at a depth of 15 km. Different one-dimensional velocity structures were tested and we present the results of two simulations performed with the velocity values given in table II. In the first model (model 1), we consider a stack of 6 km of mostly pelitic sediments ($V_p$ = 3.5 km/s, upper argillaceous Lagonegro sequence and recent deposits) overlying 5 km of carbonate platform ($V_p$ = ~ 5 km/s). A velocity contrast between the carbonate

**Table II.** Parameters for the geological units.

| Geological unit | $V_p$ (m/s) | $\nu$ | $V_s$ (m/s) |
|---|---|---|---|
| Lagonegro clays (upper sequence) and flyschs (if superficial) | 3000 | 0.33 | 1510 |
| Lagonegro clays and flyschs (if deep) | 3500 | 0.30 | 1870 |
| Lagonegro limestones and marls (lower sequence) | 5000 | 0.25 | 2890 |
| Carbonate platform | 5000 | 0.25 | 2890 |
| Crystalline basement | 7000 | 0.25 | 4040 |

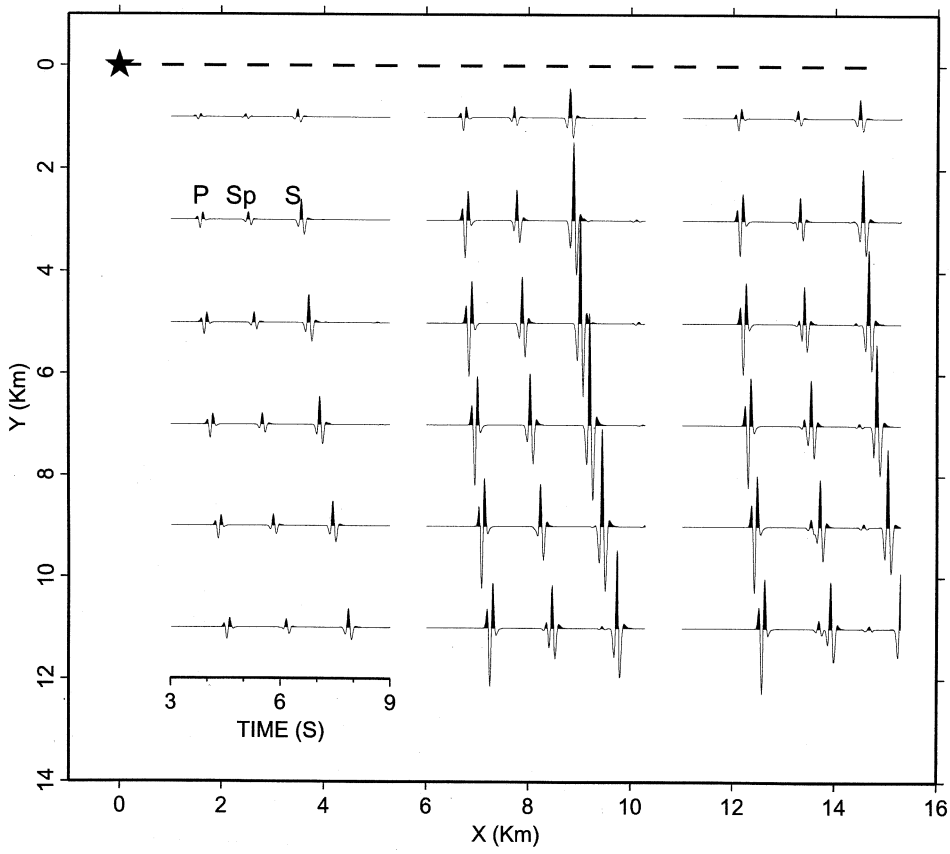


**Fig. 7a.** Synthetic seismograms (vertical component) computed for model 1 velocity and a strike-slip mechanism. Star indicates the epicentre location (see text for explanation).

platform and the deeper crystalline basement ($V_p$ = 7 km/s) has been assumed. In the second model (model 2), the first 6 km are articulated in three layers of 2 km each: a shallower pelitic unit ($V_p$ = ~ 3.0 km/s, flyschs and upper Lagonegro sequence), a middle calcareous-marly layer ($V_p$ = 5 km/s, lower Lagonegro unit) and a bottom pelitic layer ($V_p$ = ~ 3.5 km/s, upper Lagonegro sequence, flyschs and fore-deep deposits). The deeper layers are the same as in model 1. The Green functions for the vertical components of the motion were computed and convolved with a Ricker wavelet of 4 Hz.

The surface seismograms calculated at different distances from the epicentre are presented for the two models on figs. 7a,b. Looking at fig. 7a, three main phases clearly appear on the seismograms: the direct *P* and *S* waves, and the *S*-to-*P* wave converted at the top of the Ocarbonate platform. This relatively energetic phase is intermediate between the *P* and *S* waves. Its amplitude depends on the velocity contrast between the platform and the overlying formations, and particularly on the shear wave velocity in the upper sediments. Unfortunately, this parameter is not directly known as no *in situ* measurements are available. In our

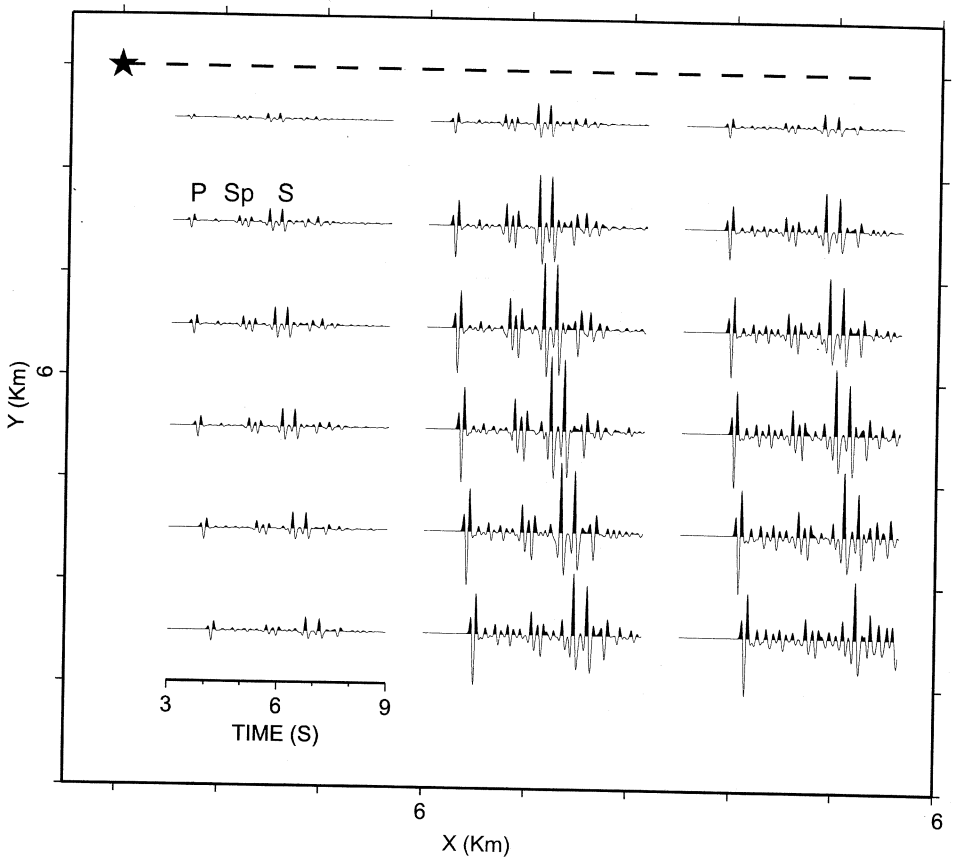


**Fig. 7b.** Synthetic seismograms (vertical component) computed for model 2 velocity and a strike-slip mechanism. Star indicates the epicentre location (see text for explanation).

study, we have assumed a Poisson coefficient of 0.25 in the Apulian platform, the lower Lagonegro sequence and the basement, and 0.3 to 0.33 in the more argillaceous units. An increase in this last value leads to a stronger *Sp* phase on the seismograms.

For the second model including the carbonatic-siliceous-marly layer of the Lagonegro formation, the seismograms (fig. 7b) appear to be more complex, as a result of the multiple reflections and refraction at the different interfaces. The *Sp* wave converted at the top of the platform is still clearly seen and still constitutes the most prominent phase between the *P* and *S* waves. The comparison between figs. 7a and 7b also shows that the delay between the *S* and *Sp* waves is shorter for the second model. This is a consequence of the presence of high-velocity layers in the sediments above the platform.

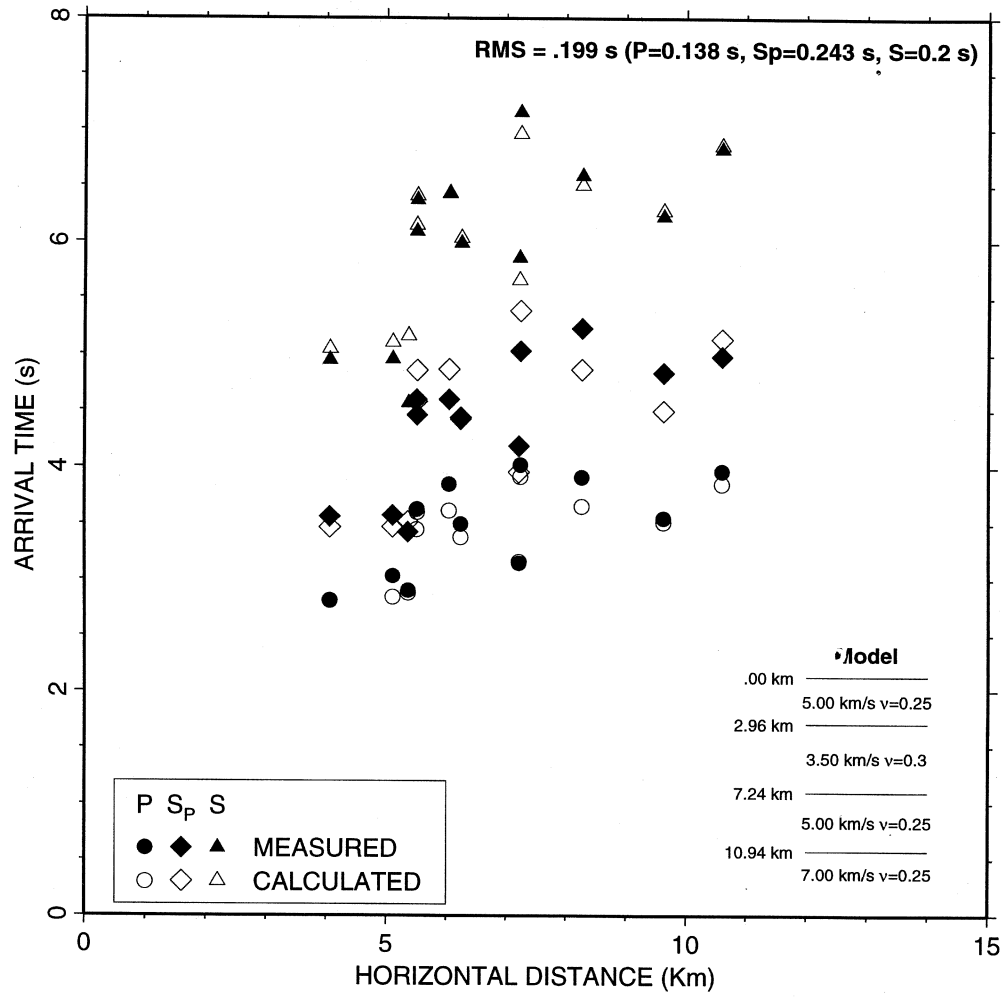


**Fig. 8.** Comparison between the observed and calculated travel times of the three phases (*P*, *Sp* and *S*) at station PIG. The bottom right corner of the graph shows the model obtained after inversion.

## 5. Data inversion

Having identified the three main phases appearing on the seismograms, we wish to obtain some information on the upper crustal structure from the travel-time data. The inversion method used here is a damped least-squares technique developed by Zelt and Smith (1992) which assumes that the structure is locally 1D. Starting from the trial velocity model, the three ray paths corresponding to the *P*, *Sp* and *S* phases are calculated, as well as the theoretical travel times and the partial derivatives. Corrections to the model parameters (velocity, thickness) were then computed considering the residuals between observed and calculated times (RMS), and new theoretical times were calculated with the updated model. This process was repeated to minimise the RMS values between observed and calculated travel-times, generally it took a few iterations. The reliability of the parameter determination may be estimated from the resolution matrix.

The inversion requires a sufficient number of observations at each station, seven stations meet this criterion (PIG, PGC, GIU, CAR, BRI, VAG and CSZ). The approximation of 1D structure is acceptable because of the short epicentral distances and the relevant depth of the earthquakes, considering also the stability of *S-Sp* times shown in fig. 5. We used model 2 as a starting model because the geological structure beneath the stations is better described by model 2 rather than model 1 (see fig. 1a,b). Through the described inversion procedure we could estimate the thickness of the different layers beneath each station considering fixed velocity values. In a second step, the results were checked studying their sensitivity to input velocity values.

The inversion process is illustrated for station PIG which shows the comparison between measured and calculated travel times at the end of the process (RMS = ~ 0.199 s). Figure 8, also shows the final model which consists of a 3 km thick layer of carbonatic-siliceous-marly Lagonegro overlying 4.3 km of pelitic sediments, above the Apulian platform. The crystalline basement was found at 11 km depth. The resolution matrix indicates that, in this case, the platform depth and the thickness of the carbonated unit of Lagonegro are well resolved for the given velocity values. Modifying slightly the velocity in the units above the platform results in a slight change in the platform depth while the relative thickness of these units varies dramatically.

The inversion process was applied to the seven stations and the depth of the carbonate platform was systematically determined with a good resolution. Figure 9 presents the platform depth as a function of *S-Sp* times. Except for station PGC, there is a good correlation between these two parameters, showing that *S-Sp* times are strongly dependent on the platform depth. Depth values range from 6 km at GIU to 8 km at CAR. Tests performed for different stations again showed that the platform depth is not very sensitive to a variation of the velocity values used in the inversion.

Some of our results may be compared to existing geological data and particularly to the EW cross-section published by Mostardini and Merlini (1986) and presented in fig. 1b. As no deep borehole data are available in the studied

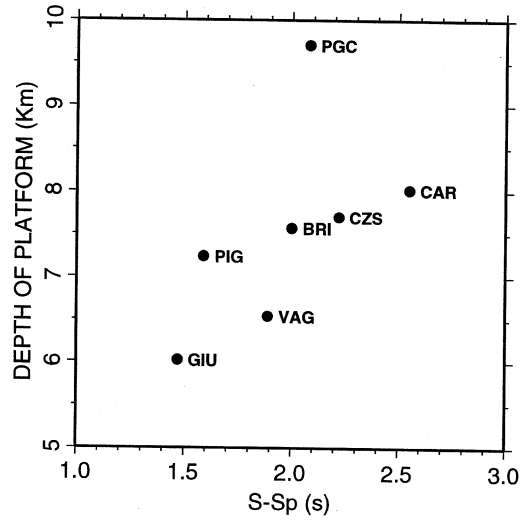


**Fig. 9.** Evolution of *S-Sp* times with the platform depth determined from one-dimensional inversion process.

area, the corresponding part of the section was drawn from superficial geological data and geophysical measurements. Two stations (PIG and BRI) are located along the cross-section. At BRI, the inversion has given a 2.7 km thick layer of carbonatic-siliceous-marly Lagonegro overlying about 5 km of pelitic unit. The upper part of the structure is consistent with the proposed cross-section. The pelitic layer is, however, thinner on the cross-section, resulting in a higher position for the Apulian platform (6.5 km depth instead of 7.5 km from the inversion).

Below station PIG, the cross-section shows 4.7 km of lower Lagonegro sequence just over the Apulian platform. On the contrary, the inversion disclosed the platform at 7.2 km depth below 3 km of carbonatic-marly Lagonegro and 4.2 km of pelitic sediments. The presence of a softer layer over the platform is supported by the existence of relatively strong converted waves. As shown by modelling, such amplitude values require a high shear modulus contrast, which may be explained by the presence of clay deposits over the platform.

## 6. Conclusions

The seismograms recorded during the Potenza sequences (1990 and 1991) exhibit three main phases: *P* and *S* waves and an intermediary phase which has been identified as a *S* to *P* wave converted at a discontinuity in the shallow crust. Seismogram analysis and 1D numerical modelling have shown that this *Sp* wave could be generated at the top of the Apulian carbonate platform which constitutes a major seismic interface in the upper crust of the Southern Apennines. The significant amplitude shown by this *Sp* converted wave requires the presence of a high shear modulus contrast and hence the presence of a Lagonegro upper unit layer overlaying the Apulian platform underneath each of the stations studied, including western ones: PIG, LIF and PGC.

The study of the travel times has shown that the delay between *S* and *Sp* waves is relatively constant at each station and could then be characteristic of the local geology. 1D inversion of the travel-time data was performed at 7 stations in order to obtain the local velocity structure. The best constrained geometric parameter during inversion is the Apulian platform depth whose values, ranging from 6 to 8 km, are consistent with published geological data in the area, even if no reliable geological or geophysical data giving accurate depth values are available to corroborate our results. The use of local seismicity and of converted waves appears to be a promising tool for investigating upper crustal structure in the Southern Apennines. In 1996 we carried out an *ad hoc* field experiment, deploying 15 three component seismic stations in the Potenza region. Based on the experience gained with this preliminary study, we are confident that the recorded earthquakes will provide more detailed information and possibly 2D or 3D geometry of the Apulian platform top.

## Acknowledgements

This work was partially supported by Fina Italiana S.A. We are grateful to Aldo Zollo and an anonymous reviewer for helpful suggestions.

*REFERENCES*

ANDERSON, H. and J. JACKSON (1987): Active tectonics of the Adriatic region, *Geophys. J. R. Astron. Soc.*, **91**, 937-987.

AZZARA, R., A. BASILI, L. BERANZOLI, C. CHIARABBA, R. DI GIOVAMBATTISTA and G. SELVAGGI (1993): The seismic sequence of Potenza (May 1990), *Ann. Geofis.*, **36** (1), 237-243.

BOUCHON, M. (1981): A simple method to calculate Green's functions for elastic layered media, *Bull. Seism. Soc. Am.*, **71**, 959-971.

D'ANDREA, S., R. PASI, G. BERTOZZI and P. DATTILO (1993): Geological model, advanced methods help unlock oil in Italy's Apennines, *Oil Gas J.*, 53-55.

DEWEY, J.F., M.L. HELMAN, E. TURCO, D.H.W. HUTTON and S.D. KNOTT (1989): Kinematics of the Western Mediterranean, in *Alpine Tectonics*, edited by M.P. COWARD, D. DIETRICH and R.G. PARK, *Geol. Soc. London, Spec. Publ.*, 265-283.

EKSTRÖM, G. (1994): Teleseismic analysis of the 1990 and 1991 earthquakes near Potenza. *Ann. Geofis.*, **37** (6), 1591-1599.

FREPOLI, A. and A. AMATO (1997): Contemporaneous extension and compression in the Northern Apennines from earthquake fault plane solutions. *Geophys. J. Int.*, **129**, 368-388.

JACOB, A.W.B. and D.C. BOOTH (1977): Observation of *Ps* reflections from the Moho, *J. Geophys.*, **93**, 687-692.

JURKEVICS, A. (1988): Polarization analysis of three-component array data, *Bull. Seism. Soc. Am.*, **78**, 1725-1743.

MALINVERNO, A. and W.B.F. RYAN (1986): Extension in the Tyrrhenian Sea and shortening in the Apennines as results of arc migration driven by sinking of the lithosphere, *Tectonics*, **5**, 227-245.

MARSELLA, E., A.W. BALLY, G. CIPITELLI, B. D'ARGENIO and G. PAPPONE (1995): Tectonic history of the Lagonegro domain and Southern Apennine thrust belt evolution, *Tectonophysics*, **252**, 307-330.

MONTONE, P., A. AMATO, A. FREPOLI, M.T. MARIUCCI and M. CESARO (1997): Crustal stress regime in Italy, *Ann. Geofis.*, **40** (3), 741-757.

MOSTARDINI, F. and S. MERLINI (1986): Appennino Centro Meridionale, sezioni geologiche e proposta di modello strutturale, *Mem. Soc. Geol. It.*, 177-202.

PATACCA, E. and P. SCANDONE (1989): Post-Tortonian mountain building in the Apennines. The role of the passive sinking of a relic lithospheric slab, in *The Lithosphere in Italy*, edited by A. BORIANI, M. BONAFEDE, G.B. PICARDO and G.B. VAI, *Accad. Naz. Lincei*, Roma, 157-176.

REGNIER, M., J.-M. CHIU, R. SMALLEY, B.L. ISACKS and M. ARAUJO (1994): Crustal thickness variation in the Andean Foreland, Argentina, from converted waves, *Bull. Seism. Soc. Am.*, **84**, 1097-1111.

ROURE, F. and W. SASSI (1995): Kinematics of deformation and petroleum system appraisal in neogene foreland fold-and-thrust belts, *Pet. Geosci.*, **1**, 253-269.

ZELT, C.A. and R.B. SMITH (1992): Seismic travel-time inversion for 2D crustal velocity structure, *Geophys. J. Int.*, **108**, 16-34.

(received January 16, 1998;
accepted March 21, 1998)